ORIGINAL ARTICLE

Molecular Genetics & Genomic Medicine
Open Access
WILEY

Phenotype–genotype correlations in a pseudodominant Stargardt disease pedigree due to a novel *ABCA4* deletion–insertion variant causing a splicing defect

Di Huang[1,2,3] (iD) | Jennifer A. Thompson[4] (iD) | Jason Charng[2] (iD) | Enid Chelva[4] (iD) | Samuel McLenachan[2] (iD) | Shang-Chih Chen[2] (iD) | Dan Zhang[2] (iD) | Terri L. McLaren[2,4] (iD) | Tina M. Lamey[2,4] (iD) | Ian J. Constable[2,5] (iD) | John N. De Roach[2,4] (iD) | May Thandar Aung-Htut[1,3] (iD) | Abbie Adams[1] (iD) | Sue Fletcher[1,3] (iD) | Steve D. Wilton[1,3] (iD) | Fred K. Chen[2,4,6,7] (iD)

[1]Centre for Molecular Medicine and Innovative Therapeutics, Murdoch University, Murdoch, Western Australia, Australia

[2]Centre for Ophthalmology and Visual Science (Incorporating Lions Eye Institute), The University of Western Australia, Nedlands, Western Australia, Australia

[3]Centre for Neuromuscular and Neurological Disorders, The University of Western Australia and Perron Institute for Neurological and Translational Science, Nedlands, Western Australia, Australia

[4]Australian Inherited Retinal Disease Registry and DNA Bank, Department of Medical Technology and Physics, Sir Charles Gairdner Hospital, Nedlands, Western Australia, Australia

[5]Department of Ophthalmology, Sir Charles Gairdner Hospital, Nedlands, Western Australia, Australia

[6]Department of Ophthalmology, Royal Perth Hospital, Perth, Western Australia, Australia

[7]Department of Ophthalmology, Perth Children's Hospital, Nedlands, Western Australia, Australia

Correspondence
Fred K. Chen, Centre for Ophthalmology and Visual Science (Incorporating Lions Eye Institute), The University of Western Australia, Perth, Western Australia, Australia.
Email: fredchen@lei.org.au

Abstract

Background: Deletion–insertion (delins) variants in the retina-specific ATP-binding cassette transporter gene, subfamily A, member 4 (*ABCA4*) accounts for <1% in Stargardt disease. The consequences of these delins variants on splicing cannot be predicted with certainty without supporting in vitro data.

Methods: Candidate *ABCA4* variants were revealed by genetic and segregation analysis of a family with pseudodominant Stargardt disease using a commercial panel and Sanger sequencing. RNA extracted from patient-derived fibroblasts was analyzed by RT-PCR to evaluate splicing behavior of the *ABCA4* variants.

Results: Affected members carrying the novel c.6031_6044delinsAGTATTTAACCAATATTT variant in exon 44 presented with contrasting phenotypes; from early-onset cone-rod dystrophy to late-onset macular dystrophy. This variant resulted in a 56-nucleotide deletion in the mutant allele by activation of a cryptic splice acceptor site which disrupts the reading frame and results in a premature termination

codon (p.Ile2003LeufsTer41). If translated, the crucial functional domains near the C-terminus would be truncated from the ABCA4 protein.

Conclusion: This work demonstrates the intrafamilial phenotypic variability in a pseudodominant Stargardt disease pedigree and the use of patient-derived fibroblasts to evaluate the effect of a novel *ABCA4* delins variant on splicing to complement in silico pathogenicity assessment.

1 | INTRODUCTION

Stargardt disease (STGD1, OMIM: 248200) is the most common form of inherited retinal disease characterized by progressive central and predominantly cone-mediated vision impairment. Mutations in *ABCA4* (MIM: 601691), encoding the adenosine triphosphate (ATP) binding cassette, subfamily A, member 4, cause a wide spectrum of retinal phenotypes that range in severity from early-onset cone-rod dystrophy to late-onset macular dystrophy (Allikmets et al., 1997; Cremers et al., 1998; Maugeri et al., 2000), depending on the combined function of the ABCA4 protein translated from the two pathogenic alleles. The ABCA4 protein is a retinoid flippase that actively transports all-*trans*-retinaldehyde and its Schiff base adduct *N*-retinyl-phosphatidylethanolamine back from the luminal (topographically equivalent to the extracellular) to the cytosolic (intracellular) leaflet of the outer segment disc membranes for reduction into all-*trans*-retinol by the various retinol dehydrogenases (Quazi, Lenevich, & Molday, 2012). A defect in the ABCA4 flippase leads to the formation of N-retinylidene-*N*-retinyl-phosphatidyl-ethanolamine (A2PE) in the lumen of the disc that is then accumulated in the retinal pigment epithelium (RPE) as it phagocytoses these bisretinoid-laden outer segments. Inside the RPE phagolysosome, A2PE is hydrolyzed to form the lipofuscin-like A2E that forms the basis of the "dark choroid" clinical sign. In addition, there are foci of photoreceptor cell degeneration resulting in the formation of subretinal autofluorescent, bisretinoid-rich flecks. Finally, cytotoxicity from these metabolites leads to confluent regions of RPE loss with secondary retinal and choriocapillaris atrophy (Braun et al., 2013; Fishman et al., 1999; Paavo, Lee, Allikmets, Tsang, & Sparrow, 2019; Stargardt, 1909).

The development of next-generation sequencing (NGS) has led to substantial progress in the discovery of the enormous number of disease-causing *ABCA4* variants. Sequencing of the entire open reading frame and adjacent intronic sequences of *ABCA4* in patients with STGD1 identifies biallelic variants in up to 60%–70%, one variant in 15%–25%, and no variants in 10%–15% of the clinically diagnosed cases (Zernant et al.,

2011, 2017). More recently, deep intronic variants are gaining recognition as potentially pathogenic changes through the creation or activation of a cryptic splice site leading to pseudo-exon inclusion (Braun et al., 2013; Zaneveld et al., 2015; Zernant et al., 2014). Despite the availability of prediction programs and published data from mini-gene assays, the precise mechanism that mediates how these variants lead to impaired flippase function remains uncertain. To further complicate matters, there is a high frequency of carriers of pathogenic *ABCA4* alleles in the general population (1.6%~10%; Huckfeldt, East, Stone, & Sohn, 2016; Jaakson et al., 2003; Yatsenko, Shroyer, Lewis, & Lupski, 2001; Zernant et al., 2011) resulting in the not infrequent observation of pseudodominant inheritance pattern in families with STGD1 (Huckfeldt et al., 2016; Lee et al., 2016; Yatsenko et al., 2001). Among the known variant types, the top three are missense variants (66%), splice site substitutions (15%) and small deletions with 20 bp or less (13%). Deletion-insertion (delins) variants are relatively rare in *ABCA4* accounting for <1% of cases (data from Human Gene Mutation Database, HGMD). Currently, there is only limited information available regarding the molecular mechanism and clinical manifestation of delins variants due to their rarity.

Here we report a novel delins variant of *ABCA4* discovered in a pseudodominant STGD1 family with extreme intrafamilial phenotypic variability. In addition to bioinformatics and in silico prediction of the variant, we also analyze *ABCA4* transcript from patient-derived fibroblasts and found that this novel delins results in an alternatively spliced *ABCA4* transcript by activation of a cryptic splice acceptor site.

2 | MATERIALS AND METHODS

2.1 | Editorial policies and ethical considerations

The study adhered to the tenets of the Declaration of Helsinki and ethics approval was obtained from the Human Ethics Office of Research Enterprise, The University of Western Australia

(RA/4/1/8932 and RA/4/1/7916) and the Human Research Ethics Committee, Sir Charles Gairdner Hospital (2001-053), Perth, Western Australia, Australia. Written informed consent was obtained from all participants. The use of human cells for this research was approved by the Murdoch University Human Research Ethics Committee, approved number 2017_101.

2.2 | Clinical assessment and tissue biobanking

Clinical history and full ophthalmic examination, including best-corrected visual acuity (VA) using the Early Treatment of Diabetic Retinopathy Study (ETDRS) letter chart and dilated fundus examination were undertaken for all available family members. Members of this family with STGD1 were monitored using a standardized imaging protocol. Multimodal retinal imaging included (a) ultra-wide field color fundus photography, green-light autofluorescence (AF) imaging (P200Tx and California, Optos plc), (b) 30° and 55° scanning laser ophthalmoscopy, including near-infrared reflectance (NIR), blue-light and near-infrared AF, and (c) spectral domain optical coherence tomography (SD-OCT, Spectralis OCT2 and Spectralis HRA2, Heidelberg Engineering). The Macular Integrity Assessment (MAIA, CenterVue) was used to evaluate macular function. Electrophysiology (electro-oculography, full-field electroretinography [ERG] and pattern ERG; LKC UTAS E-3000, Maddison, USA/ RETIport 3.2, Roland Consult) was performed according to the International Society for Clinical Electrophysiology of Vision (ISCEV) standards (Bach et al., 2013; Constable et al., 2017; McCulloch et al., 2015). Clinical results for the right eye were reported given that the two eyes were generally symmetrical. Interpretation of the full-field ERG was based on age-matched controls ($n = 49$ in LKC/34 in RETIport).

All family members were invited to provide peripheral blood or saliva samples for genetic analysis. DNA was extracted from peripheral blood or saliva samples, collected and stored as detailed previously (De Roach et al., 2013). Control dermal fibroblasts were cultured from skin biopsies taken from individuals with no ocular history aged 63 (HC#1) and 28 (HC#2). Skin biopsies from family members were obtained for dermal fibroblast culture and transcript analysis. A 3-mm punch biopsy of the dermis in the dorsal skin of the upper arm was performed after local anesthetic infiltration with 1% lignocaine. Biopsies were then seeded into a six-well plate with Dulbecco's-Modified Eagle Medium, DMEM (Cat. No. 11995115, Thermo Fisher Scientific) supplemented with 10% sterile fetal bovine serum, FBS (Cat. No. SFBS-AU, Bovogen Biologicals) and 1% antibiotic-antimycotic (Cat. No. 15240062, Thermo Fisher Scientific). The cell culture media was changed 2–3 times every week. After 3–5 weeks of culture, the fibroblasts isolated from biopsies

were collected and transferred into a T75 flask for larger scale expansion. Aliquots of approximately 1 million cells, with cell culture media supplemented with 10% Dimethyl sulfoxide (Cat. No. D2650, Sigma-Aldrich), were stored in liquid nitrogen until use.

2.3 | Genetic and pathogenicity analyses

Genomic DNA was analyzed in three siblings by targeted NGS, using one of two versions of the Stargardt/Macular dystrophy panel (2014 version; 5 genes or 2019 version; 14 genes) or the retinal dystrophy (RD) NGS SmartPanel (version 11; 280 genes; Chiang et al., 2015) targeting all exons and flanking intronic regions of known retinal dystrophy genes, together with known *ABCA4* deep-intronic variants. Candidate variants were confirmed by Sanger sequencing. Sequencing was performed by Casey Eye Institute Molecular Diagnostics Laboratory or Molecular Vision Laboratory. Sequences were aligned to the *ABCA4* reference sequence NG_009073.1 (NM_000350.2/3), with nucleotide 1 corresponding to the A of the start codon ATG, and described in accordance with Human Genome Variation Society recommendations version 15.11 (den Dunnen, 2016). The phase of the variants was examined in the father and the siblings. Variant pathogenicity was assessed as previously described (Thompson et al., 2017) and interpreted according to the American College of Medical Genetics and Genomics/ Association for Molecular Pathology (ACMG/AMP) joint guidelines (Richards et al., 2015).

The predicted effect on splicing was sought using the five algorithms (SpliceSiteFinder-like, MaxEntScan, NNSPLICE, GeneSplicer, and ESEfinder) provided by the Interactive Biosoftware Alamut® software (Cartegni, Wang, Zhu, Zhang, & Krainer, 2003; Pertea, Lin, & Salzberg, 2001; Reese, Eeckman, Kulp, & Haussler, 1997; Yeo & Burge, 2004; Zhang, 1998; Alamut Visual 2.11.0 software package, http:// www.interactive-biosoftware.com/alamut-visual/). Mutation Taster (Schwarz, Cooper, Schuelke, & Seelow, 2014; http:// www.mutationtaster.org/) was used to re-assess the splicing defect caused by the delins variant. Protein structure was predicted using I-TASSER tools (Zhang, 2008; https://zhanglab. ccmb.med.umich.edu/I-TASSER/, an online server updated on 2019/06/13) and the figure of the predicted protein structure was processed using PyMOL software (DeLano, 2002; PyMOL 2.3.0, http://pymol.org).

2.4 | RNA isolation and *ABCA4* transcript analyses

Patient-derived fibroblasts were resurrected and cultured in DMEM (Cat. No. 11995065, Thermo Fisher Scientific)

supplemented with 10% FBS (Cat. No. WS-FBS-AU-015, Fisher Biotec, SERANA) and 1x GlutaMax (Cat. No. 35050061 Thermo Fisher Scientific). Total RNA was isolated from fibroblasts obtained from STGD1 patients and healthy controls using MagMAX™-96 Total RNA Isolation kit (Cat. No. AM1830, Thermo Fisher Scientific), following the manufacturer's protocol. RNA was quantified by ND-1000 Spectrophotometer (Thermo Fisher Scientific) and stored at −20°C until use.

RT-PCR was performed using 50 ng of total RNA, 8 μM of each primer pair (Table S1), and one-step SuperScript III one step RT-PCR kit with reverse transcriptase and Platinum *Taq* DNA polymerase (Cat. No. 12574026, Invitrogen, Thermo Fisher Scientific) according to the manufacturer's instructions. RT-PCR conditions for *ABCA4* transcripts from exons 41 to 46 included 55°C for 30 min and 94°C for 2 min (cDNA synthesis), followed by 33 cycles of 30 s at 94°C (denaturation), 1 min at 64°C (annealing), and 2 min at 68°C (extension). The annealing temperatures for *ABCA4* amplification from exons 30 to 33 and exon 38 to 43 were at 65°C and 62°C, respectively, and PCRs were performed for 32 and 35 cycles, respectively. The integrin alpha 4 (*ITGA4*) transcript product was used as a loading control. The RT-PCR conditions for *ITGA4* transcripts amplification were the same as above, except the annealing temperature was 55°C and PCR was performed for 25 cycles. A quantity of 4 μl of the *ABCA4* and *ITGA4* RT-PCR reactions was resolved on a 2% (weight/volume) agarose gel. Images were captured using the Fusion FX gel documentation system (Vilber Lourmat). Image processing was performed for the entire image. The identities of PCR products were confirmed by bandstab purification (Wilton, Lim, Dye, & Laing, 1997) and Sanger sequencing (Australian Genome Research Facility). For semi-quantitative estimation of aberrantly spliced products, the band intensities were determined using Image J (NIH) software. The percentage of aberrantly spliced and full-length products of the patients relative to total transcripts of healthy controls were calculated according to (aberrantly spliced/total transcripts) and (full-length/total transcripts).

3 | RESULTS

3.1 | Clinical presentation and phenotype of the proband and his parents

The proband (II:4, Figure 1) presented at the age of 50 with central visual impairment in the right eye due to a subfoveal vitelliform lesion associated with pattern macular dystrophy. His presenting VA was 20/20 in both eyes. By the age of 53, VA in the right eye declined to 20/40 but the left eye remained at 20/20. Multiple linear and branching hyperautofluorescent subretinal deposits and extrafoveal RPE atrophy were present in both eyes (Figure 2, right eye shown). Fluorescein angiography showed a butterfly pattern of masking by the linear yellow deposits, window defects from RPE atrophy and a lack of the "dark choroid" sign. Microperimetry demonstrated overall reduced retinal sensitivity and dense scotoma in the region of RPE atrophy (Figure S1). Electrophysiology (ISCEV 2016) showed normal Arden ratio, dark- and light-adapted full-field ERG responses, albeit at the lower limits of normal range (Figure S2). Pattern ERG and dark adaptometry were normal. Over a 3-year follow-up period, his VA in the right eye improved to 20/30 as the subfoveal deposit was reabsorbed and replaced by a small patch of juxtafoveal RPE atrophy.

The proband's mother (I:2) presented to our practice for a second opinion at the age of 68 with a 2-year history of central visual loss in both eyes due to pattern macular dystrophy. At the first visit, her VA was 20/30 and 20/60 in right and left eyes, respectively. She also had bilateral fishtail-like flecks in the macular region resembling the proband's phenotype and her fluorescein angiography also showed a lack of the "dark choroid" sign (Figure S3). Electrophysiology (ISCEV 2001) showed normal Arden ratios and both dark- and light-adapted full-field ERG responses were within normal limits (Figure S2). Pattern ERG was also within normal limits and the Farnsworth 100 Hue test was normal. The proband's mother (I:2) passed away at the age of 73. The proband's asymptomatic father (I:1) had a history of bilateral cataract surgery and VA was 20/20 at the age of 85. Macula and optic nerves were normal on clinical examination and OCT and widefield fundus AF imaging were unremarkable at presentation and 4 years later at age 89 (Figure 2, right eye shown). MAIA Microperimetry at the age of 89 demonstrated macular retinal thresholds within the normal range (Figure S4).

3.2 | Clinical presentation and phenotype of the proband's three siblings

The proband has two older brothers (II:1 and II:3) with early-onset STGD1, while his sister (II:2) is asymptomatic (Figure 1).

The first and the oldest affected brother (II:1) presented to our practice at age 17 with a history of progressive vision loss from age 7 and was diagnosed with "functional visual loss" at age 10. His acuity at age 17 was 20/120 in both eyes with diffuse fine pigmentation in the macula surrounded by fine yellow flecks. Electrophysiology (pre-ISCEV standard era) at age 17 showed normal light-adapted ERG responses and a reduced Arden ratio of 1.3 (Figure S5). By the age of 20, his VA had declined to 20/200 in both eyes. From the age of 46, his VA was 20/600 in both eyes and remained unchanged at age 60. OCT showed significant outer retinal atrophy with large areas of RPE loss in the posterior pole
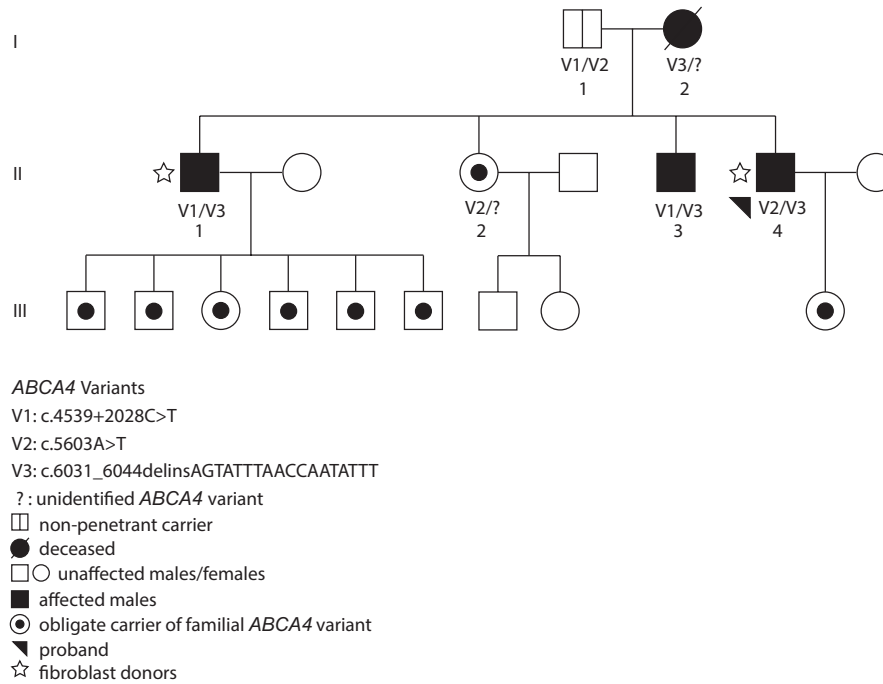
ABCA4 Variants
V1: c.4539+2028C>T
V2: c.5603A>T
V3: c.6031_6044delinsAGTATTTAACCAATATTT
? : unidentified *ABCA4* variant
⬚ non-penetrant carrier
● deceased
□○ unaffected males/females
■ affected males
⊙ obligate carrier of familial *ABCA4* variant
◣ proband
☆ fibroblast donors

FIGURE 1 Pedigree showing members of a family affected by Stargardt disease (STGD1) with pseudodominant inheritance. II:4 was the proband with late-onset (50 years old), pattern-like macular dystrophy that was phenotypically distinct from II:1, who presented with early-onset (8 years old) cone-rod dystrophy. The other brother (II:3) of the proband presented symptoms at the age of 15 and had impaired best-corrected visual acuity in both eyes at age 6. The proband's mother (I:2) has an almost identical phenotype to the proband. His father (I:1) and sister (II:2) are both asymptomatic with no retinal lesion despite carrying two pathogenic alleles, V1 and V2; and V2 and an unidentified variant, respectively

sparing the peripapillary region (Figure 2). Heterogeneous AF signal outside the macular atrophy extended anterior to the equator (Figure 2). Follow-up electrophysiology (ISCEV 2016) at the age of 57 showed profoundly reduced dark- and light-adapted full-field and pattern ERG responses (Figure S2).

The second affected brother (II:3) presented at the age of 15 to the same practice, with a history of strabismus operations at age 3 and 7 years and poor vision despite spectacle correction from the age of 6. His presenting VA was 20/60 and 20/120 in right and left eyes respectively with no obvious fundal lesions. Electrophysiology (pre-ISCEV era) also showed a reduced Arden ratio of 1.5 and full-field ERG was not performed. Fluorescein angiography showed a central region of stippled hyperfluorescence with no peripheral lesions. The presence of dark choroid was not specifically mentioned. By age 18, his VA had declined to 20/200 in both eyes. At age 46, his VA declined to 20/600 in both eyes due to extensive retinal atrophy. By the age of 58, his VA reduced to finger counting only in both eyes.

The proband's unaffected sister (II:2) was examined at the age of 56 with no visual symptoms. Her VA was 20/20 in both eyes and there was no fundal lesion. Both OCT and widefield Optos AF were within normal limits at presentation and at follow-up 4 years later (Figure 2). MAIA Microperimetry at the age of 60 demonstrated macular retinal thresholds within the normal range (Figure S4).

3.3 | Genetic diagnoses

Three of the four potential candidate *ABCA4* variants were detected independently in three separate NGS panels (c.4539+2028C>T/p.?, c.6031_6044delinsAGTATTTAACCAATATTT/p.(Ile2003LeufsTer41) [deletion of 14 nucleotides and insertion of 18 nucleotides, a net gain of 4 nucleotides] and c.5603A>T/p.(Asn1868Ile)), and shown by Sanger sequencing to segregate with disease in this pedigree. One of these panels, used for the asymptomatic II:2, revealed four variants with high allele frequencies: c.[4774-17_4774-16delGT] (maternal[M]) and c.[1356+10dupG, 4203C>A and 5603A>T] (paternal[P]) and thus was not informative for the unidentified maternal pathogenic variant that contributes to the pattern macular dystrophy.

The parental genotypes were identified as c.[4539+2028C>T/p.?];[5603A>T/p.(Asn1868Ile)][P] and c.[6031_6044delins18/p.(Ile2003LeufsTer41)]; [unidentified][M]. II:1 and II:3 are compound heterozygous for c.4539+2028C>T[P]/p.? and c.6031_6044delins18[M]/p.(Ile2003LeufsTer41), and II:4 is compound heterozygous for c.5603A>T[P]/p.(Asn1868Ile) and c.6031_6044delins-18[M]/p.(Ile2003 LeufsTer41). The unaffected sibling II:2 is compound heterozygous for c.5603A>T[P]/p.(Asn1868Ile) and an unidentified maternal pathogenic variant (Figure 1). Pathogenicity assessment of the respective variants indicated they may be pathogenic (Table S1). On this basis, these
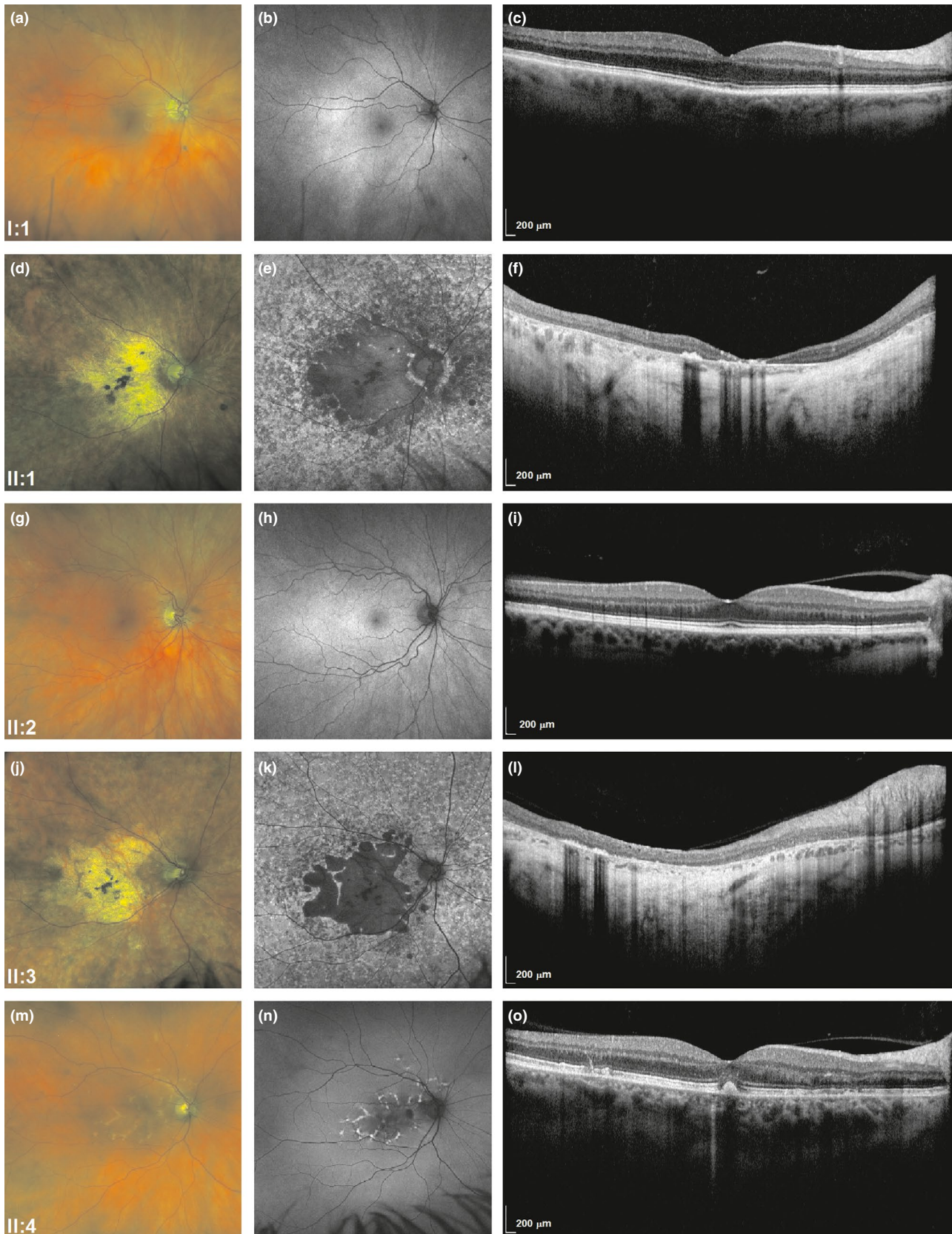
FIGURE 2 Fundus color photographs, fundus autofluorescence, and optical coherence tomography (OCT) scans of the right eyes of the family members including the father (I:1, a–c), the oldest brother (II:1, d–f), the sister (II:2, g–i), the other brother (II:3, j–l) and the proband (II:4, m–o). II:1 and II:3 had extensive atrophy in the macular region with loss of central autofluorescence and outer nuclear layers. II:4 had fish tail fleck-like lesions in the foveal and parafoveal regions which corresponded to focal subretinal deposits. Scale bars = 200 μm as shown in OCT scans
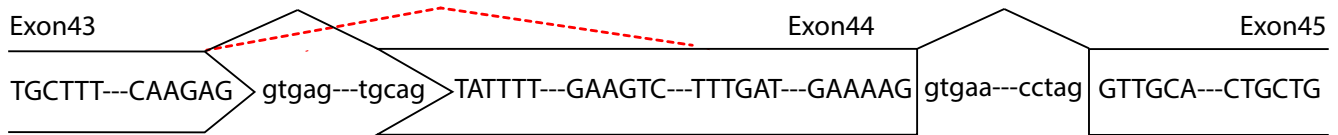
FIGURE 3 In silico prediction of the splicing effect caused by c.6031_6044delins18[M]/p.(Ile2003LeufsTer41) mutation. Schematic representation of partial exon 43, complete exon 44 and partial exon 45 of *ABCA4* transcript, identifying the location of c.6031_6044delins18[M]. The black lines show normal splicing from the canonical splice sites and the red dash lines show the aberrant splicing caused by c.6031_6044delins18[M]. The predicted value of the splice acceptor sites (small green rectangles) increased in the mutant sequence compared to the reference sequence. The cryptic splice acceptor site created by c.6031_6044delins18[M] is indicated by the red asterisk. The effect of the variant on exonic splicing enhancer (ESE) including eliminating, weakening and creating a new ESE is predicted using Alamut visual (http://www.interactive-biosoftware.com/alamut-visual/)

variants were considered the most likely candidates for disease in these cases.

3.4 | In silico prediction of aberrant splicing in the three candidate *ABCA4* variants

According to the predictions provided by Alamut® software, a cryptic splice acceptor site at *ABCA4* c.6058 (exon 44) that includes the canonical "AG" splice acceptor site sequence is strongly activated by the c.6031_6044delins 18[M]/p.(Ile2003LeufsTer41) variant (Figure 3). Further in silico predictions showed that the c.6031_6044delins18[M]/p.

(Ile2003LeufsTer41) variant creates a new SRp40 motif, while weakening an exonic splicing enhancer SC35 and eliminating the SRp55 motif. ABCA4 mutant transcripts utilizing the activated splice acceptor site have a reading frameshift that results in a premature termination codon in exon 45 (p.Ile2003LeufsTer41) which, according to Mutation Taster (Table S2), predicted NMD of the mutant mRNA.

In silico analysis of the c.4539+2028C>T/p.? and c.5603A>T/p.(Asn1868Ile) variants on the *ABCA4* transcript splicing was also performed and predicted that the c.4539+2028C>T[P]/p.? creates new SC35 and SRp40 splice motifs, while no significant alterations in splicing is predicted due to the c.5603A>T[P]/p.(Asn1868Ile) variant (data
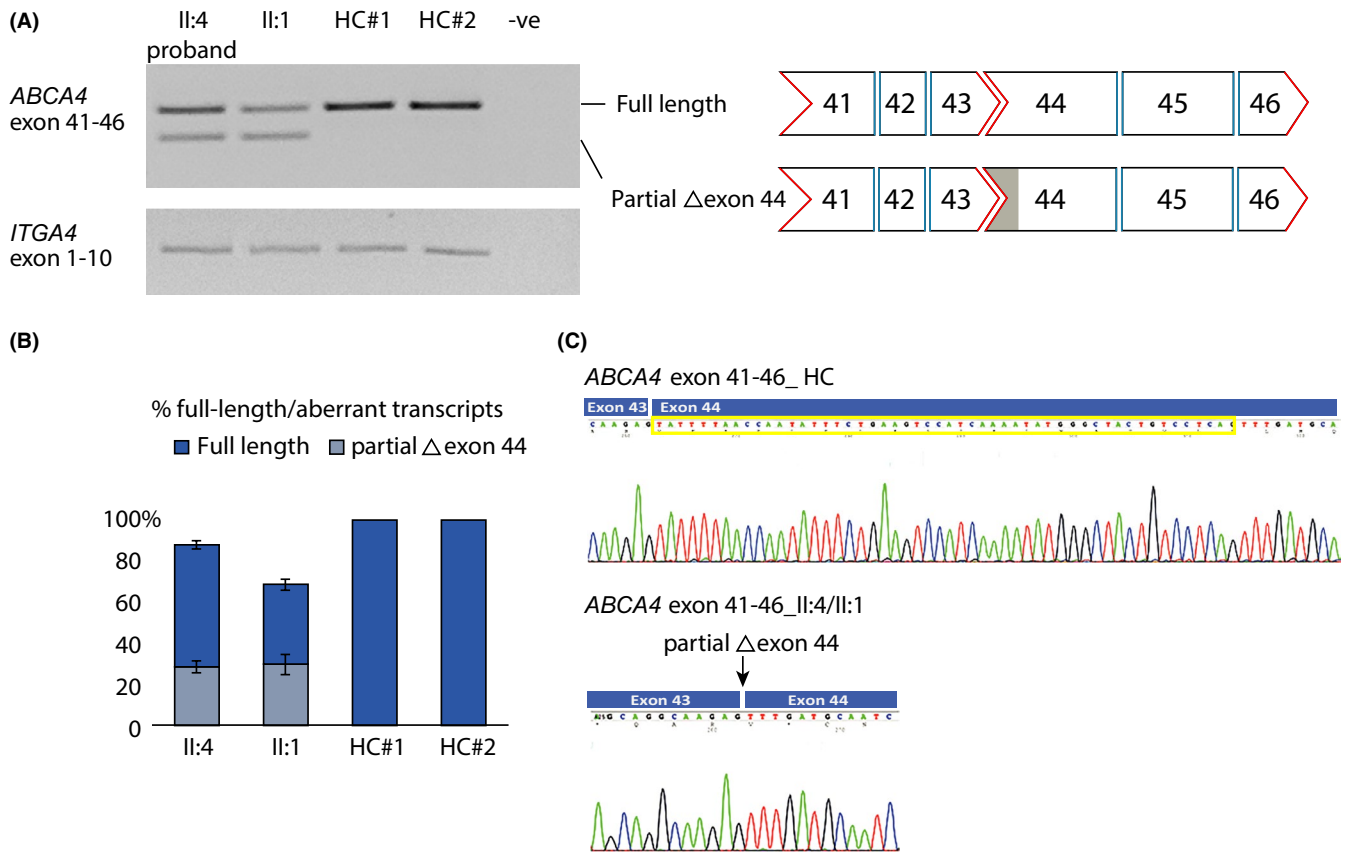
FIGURE 4 Identification of aberrantly spliced transcripts caused by the *ABCA4* c.6031_6044delins18^M/p.(Ile2003LeufsTer41) mutant allele. (a) RT-PCR analysis showing the *ABCA4* mRNA isoforms encompassing *ABCA4* exons 41–46 in fibroblasts derived from two patients heterozygous for the c.6031_6044delins18^M allele (II:4, the proband; and II:1) and from two healthy control lines (HC#1 and HC#2). Aberrantly spliced products with partial deletion of exon 44 were detected in both II:4 and II:1-derived fibroblasts. *ITGA4* was used as a positive RT-PCR internal control. −ve: RT-PCR negative control. (b) Stacking bar graph depicts the percentage of the normal and the aberrant splice isoforms relative to healthy controls on the gel shown in part A. An average value of three independent experiments are shown. Error bars indicate standard deviation. (c) Chromatogram of Sanger sequencing confirmed the 56-nucleotide deletion in the mutant allele caused by c.6031_6044delins18^M. HC, healthy controls; *ITGA4*, integrin alpha 4; Δ, deletion

not shown). This variant has been previously regarded as hypomorphic due to its mild effect and high allele frequency in the normal population (Runhart et al., 2018; Zernant et al., 2017).

3.5 | *ABCA4* transcript analysis in patient fibroblasts

The in silico prediction of aberrant splicing was further evaluated by examining splicing defects of *ABCA4* transcripts in patient fibroblast strains generated from the proband II:4 (c.[5063A>T^P];[6031_6044delins18^M/p.(Ile2003LeufsTer41)]) and his oldest brother II:1 (c.[4539 + 2028C>T^P/p.?];[6031_6044delins18 ^{M}/p.(Ile2003LeufsTer41)]). Semi-quantitative RT-PCR amplification of *ABCA4* transcripts from fibroblasts derived from these two patients and the two controls showed a consistent full-length product of 627 bp, corresponding to the correctly spliced products encompassing

exon 41 to exon 46. The level of the full-length transcripts of the two patients was reduced compared to healthy controls. An additional smaller amplicon, accounting for approximately 30% of the total *ABCA4* transcript was observed in both II:1 and II:4 derived fibroblasts but not in the control lines (Figure 4). Sanger sequencing showed that the smaller amplicon resulted from a deletion of 56 nucleotides in exon 44 of the mutant allele, confirming their origin from the common c.6031_6044delins18^M/p.(Ile2003LeufsTer41) allele carried by II:1 and II:4 (Figure 4c).

To investigate the effects of the different paternal alleles (*ABCA4* c.4539+2028C>T^P/p.? and c.5603A > T^P/p.(Asn1868Ile)) carried by II:1 and II:4 on *ABCA4* pre-mRNA splicing, we amplified the *ABCA4* transcript from exons 30 to 33 and exons 38 to 43, respectively. Only full-length products of 346 bp (amplified from exons 30 to 33) or 544 bp (amplified from exons 38 to 43) were observed in both patient fibroblasts and healthy controls (data not shown). Validation of the amplicons by Sanger sequencing showed that both the
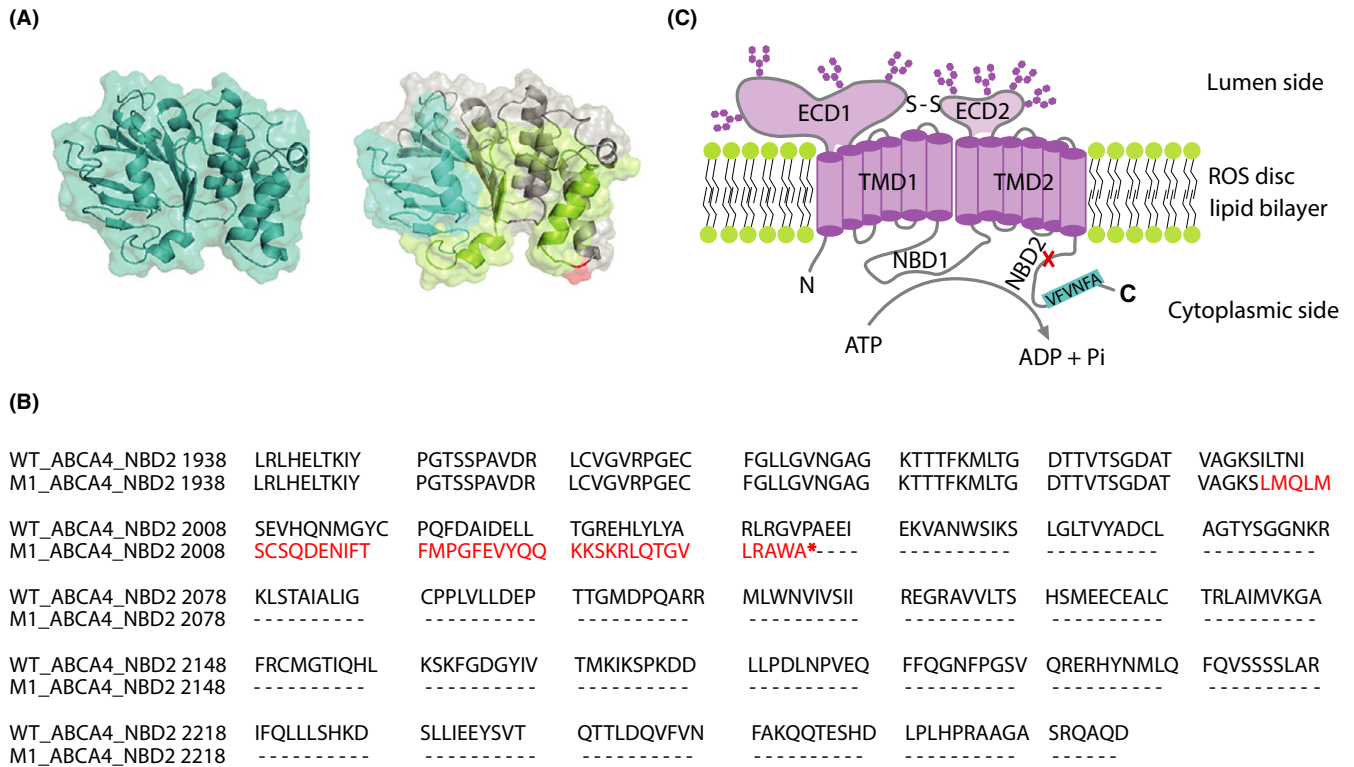
(A)

(C)

(B)

WT_ABCA4_NBD2 1938	LRLHELTKIY	PGTSSPAVDR	LCVGVRPGEC	FGLLGVNGAG	KTTTFKMLTG	DTTVTSGDAT	VAGKSILTNI
M1_ABCA4_NBD2 1938	LRLHELTKIY	PGTSSPAVDR	LCVGVRPGEC	FGLLGVNGAG	KTTTFKMLTG	DTTVTSGDAT	VAGKSLMQLM
WT_ABCA4_NBD2 2008	SEVHQNMGYC	PQFDAIDELL	TGREHLYLYA	RLRGVPAEEI	EKVANWSIKS	LGLTVYADCL	AGTYSGGNKR
M1_ABCA4_NBD2 2008	SCSQDENIFT	FMPGFEVYQQ	KKSKRLQTGV	LRAWA*----	----------	----------	----------
WT_ABCA4_NBD2 2078	KLSTAIALIG	CPPLVLLDEP	TTGMDPQARR	MLWNVIVSII	REGRAVVLTS	HSMEECEALC	TRLAIMVKGA
M1_ABCA4_NBD2 2078	----------	----------	----------	----------	----------	----------	----------
WT_ABCA4_NBD2 2148	FRCMGTIQHL	KSKFGDGYIV	TMKIKSPKDD	LLPDLNPVEQ	FFQGNFPGSV	QRERHYNMLQ	FQVSSSSLAR
M1_ABCA4_NBD2 2148	----------	----------	----------	----------	----------	----------	----------
WT_ABCA4_NBD2 2218	IFQLLLSHKD	SLLIEEYSVT	QTTLDQVFVN	FAKQQTESHD	LPLHPRAAGA	SRQAQD	
M1_ABCA4_NBD2 2218	----------	----------	----------	----------	----------	------	

FIGURE 5 Protein modeling, topologic organization and sequence alignments of wild-type and mutant protein on the assumption that transcripts from the c.6031_6044delins18^M/p.(Ile2003LeufsTer41) escape nonsense-mediated decay (NMD). (a) An overview of the nucleotide-binding domain 2 (NBD2) of the ABCA4 protein based on homology modeling using the known crystal structure of *Thermotoga maritima* (protein data bank ID:1VPL, identity: 31.2%) obtained from I-TASSER server. NBD2 of wild-type (left) and unaffected region in mutant (right) are colored cyan. The PTC caused by the c.6031_6044delins18^M is indicated in red. The sequences before the PTC (fluorescent green), containing alpha-helix and beta-strands, are different from the wild-type due to the frameshift. The sequences after the PTC (gray) are eliminated in the mutant protein. The translucent shadow provided as a background to the sequence indicates spatial structure changes in mutant protein (multi-color) compared to wild-type (cyan). The figure was prepared using Pymol software. (b) Protein sequence alignment displays the amino acids in the latter part of the ABCA4 protein. Normal sequences of ABCA4 are shown in black, amino acid changes are colored red. Termination is indicated with an asterisk and short horizontal lines represent untranslated amino acids. (c) Topological model of the wild-type human ABCA4 protein, modified from (Molday, Zhong, & Quazi, 2009). The termination codon is indicated by the red cross and the "VFVNFA" motif located near the C-terminus of the ABCA4 protein is highlighted in blue. ADP, adenosine diphosphate; ATP, adenosine triphosphate; ECD, extracytoplasmic domain; NBD, nucleotide-binding domain; NMD, nonsense-mediated decay; Pi, inorganic phosphate; PTC, premature termination codon; ROS, rod outer segment; S-S, disulfide bond; TMD, transmembrane domain

346 bp and 544 bp amplicons were canonically spliced products, indicating that no alternative splice sites were activated by c.4539+2028C>T^P/p.? or c.5603A>T^P/p.(Asn1868Ile), in contrast to that predicted in silico.

3.6 | Predicted protein alterations due to the *ABCA4* c.6031_6044delins18^M/p.(Ile2003Leufs Ter41) variant

The delins will result in a frameshift in the mature mRNA such that 89 bases from exon 44 and 34 bases from exon 45 will be mistranslated until a UGA termination codon is encountered. The additional 40 amino acids and the loss of those encoded by the downstream 6 exons would seriously compromise protein function. A superimposed homology model of the nucleotide-binding domain 2 (NBD2) constructed by I-TASSER tools showed that the premature termination codon leads to total loss of 231 amino acid residues, including the latter portion of the NBD2 (Figure 5).

4 | DISCUSSION

We described a unique pseudodominant STGD1 pedigree with extremes of retinal phenotypes, from severe cone-rod dystrophy to late-onset macular dystrophy across two generations. Genetic diagnosis revealed a novel heterozygous *ABCA4* c.6031_6044delins18^M/p.(Ile2003LeufsTer41) variant. We showed that the novel variant results in the deletion of 56 nucleotides in the mutant allele in a proportion of *ABCA4* transcripts from patient-derived fibroblasts.

The STGD1 phenotype is a continuum that lies between early-onset cone-rod dystrophy and late-onset macular dystrophy. Early-onset STGD1 is typically characterized by early foveal impairment within the first decade and the rapid loss of central visual function during the second decade of life. This severe subtype often presents with the absence of obvious fundal abnormalities or only subtle flecks in the early stages (Lambertus et al., 2015). In our study, the early and rapid progressive vision loss, the severe outer retinal atrophy associated with large areas of RPE loss in the posterior pole and the generalized light- and dark-adapted retinal dysfunction on ERG in the two older brothers (II:1 & II:3) are consistent with the early-onset cone-rod dystrophy phenotype. This childhood-onset retinal dystrophy converges to a single clinical and functional endpoint characterized by profound chorioretinal atrophy and severe central and peripheral vision loss (Lambertus et al., 2015). In contrast, late-onset STGD1, with better presenting VA owing to foveal sparing and a slower progression of vision loss, is increasingly recognized as the mild end of the spectrum of _ABCA4_-associated retinopathy (Westeneng-van Haaften et al., 2012). The proband (II:4) and his mother (I:2) had a relatively preserved VA, isolated macular dysfunction (normal full-field ERG), larger vitelliform-like lesions with relatively slow rate of progression, exhibiting features that are consistent with the phenotype of late-onset STGD1 reported previously (Tanna, Strauss, Fujinami, & Michaelides, 2017; Westeneng-van Haaften et al., 2012). Interestingly, the father of the proband carrying biallelic pathogenic and hypomorphic variants had no retinal dystrophy phenotype based on multimodal imaging even at the age of 89 (see below for further discussion).

4.1 | Contrasting phenotypes due to different paternal alleles

There is increasing evidence that the age of onset of STGD1 correlates to the severity of the underlying _ABCA4_ variants, with the early-onset phenotype being associated with more deleterious variants on both alleles compared to the late-onset "foveal-sparing" STGD1 (Lambertus et al., 2015; Tanna et al., 2017; Westeneng-van Haaften et al., 2012; Yatsenko et al., 2001). In this study, the STGD1 family exhibited extreme intrafamilial phenotypic variability. In view of the 3 brothers carrying a common c.6031_6044delins18[M]/p. (Ile2003LeufsTer41), it can be hypothesized that the phenotypic variability between II:1/II:3 and II:4 is primarily due to the differences between the c.4539+2028C>T[P]/p.? and c.5603A>T[P]/p.(Asn1868Ile) variants.

We reviewed all published literature on STGD1 individuals carrying either c.4539+2028C>T[P]/p.? or c.5603A>T-[P]/p.(Asn1868Ile) as the second _ABCA4_ allelic variant. The c.4539+2028C>T[P]/p.?, located in intron 30, was initially

reported in a cohort by Braun and colleagues (Braun et al., 2013) and thus far has been identified in 13 case individuals (Braun et al., 2013; Lee et al., 2016; Schulz et al., 2017; Zernant et al., 2014). According to predictive programs, it has no effect on splicing based on predicted changes to cryptic splice sites (rather than exonic splicing enhancer; Zernant et al., 2014). In our experiment, we did not detect any additional splicing products in patient-derived fibroblasts using primers amplifying _ABCA4_ from exons 30 to 33. This is consistent with the result from Albert et al., who demonstrated a lack of aberrant spliced products in fibroblasts from individuals harboring c.4539+2028C>T (Albert et al., 2018). However, in patient fibroblast-derived induced pluripotent stem cells and photoreceptor precursor cells, c.4539+2028C>T resulted in a 345-nucleotide pseudo-exon insertion in a proportion (~12.5%) of the _ABCA4_ transcripts that was thought to undergo NMD (Albert et al., 2018). The disparate results indicate a tissue-specific pattern of _ABCA4_ splicing and underscore the importance of using retinal tissue to analyze the effects of _ABCA4_ variants. The c.5603A>T[P]/p. (Asn1868Ile) variant, a frequently occurring _ABCA4_ variant (minor allele frequency ~6.6% in the general population) previously considered benign, is now considered hypomorphic and therefore pathogenic under certain circumstances (Zernant et al., 2017, 2018). It accounts for approximately 80% of late-onset STGD1 cases in a US cohort and results in a distinct clinical phenotype, including foveal sparing (Zernant et al., 2017). In this pedigree, II:1 and II:3 manifested earlier onset and more severe STGD1 phenotypes compared to II:4, suggesting that c.4539+2028C>T[P]/p.? is more deleterious than c.5603A>T[P]/p.(Asn1868Ile) in lowering levels of the functional ABCA4 protein function.

4.2 | Variable penetrance of ABCA4 c.5603A>T/p.(Asn1868Ile) and unidentified hypomorphic alleles

Interestingly, the non-penetrant father (I:1) and sister (II:2) are proven, and obligate, carriers of two disease-causing _ABCA4_ variants, respectively. The proband's father, carrying c.4539+2028C>T[P]/p.? and c.5603A>T[P]/p.(Asn1868Ile), remained unaffected at age 89, similar to the asymptomatic cases recorded in a previous study that attributed this phenomenon to the low penetrance (less than 5%) of _ABCA4_ c.5603A>T when in _trans_ configuration with a severe variant (Runhart et al., 2018). In the case of the proband's sister (II:2), failure to detect the other unidentified maternal _ABCA4_ variant is not unexpected given the hypermutability of this gene and the possibility of many other hypomorphic or intronic variants that are still yet to be described. The absence of retinal lesions or macular dysfunction at the age of 60 does not rule out an extremely late-onset STGD1. However, in addition to

the late onset of disease and the milder phenotype evident in the proband's mother, this finding is an indication that the unidentified maternal *ABCA4* variant is also mild or hypomorphic. Factors other than severity of the variants, such as environmental exposure, developmental events and underlying modifier genes, may also contribute to this extreme intrafamilial phenotype (Lois, Holder, Fitzke, Plant, & Bird, 1999; Runhart et al., 2018; Schindler et al., 2010). Pseudodominant transmission of STGD1 is not unexpected given the high carrier rate of pathogenic *ABCA4* alleles, which has been estimated to occur in 1.6% to up to 10% of the population (Huckfeldt et al., 2016; Jaakson et al., 2003; Yatsenko et al., 2001; Zernant et al., 2011). The frequency would be even higher with the contribution of yet-to-be-discovered, noncoding variants. The range of frequencies would seem to be at odds with the estimated prevalence of STGD1 of 1 in 10,000 that was attributed to incorrect interpretation of a large number of more common *ABCA4* variants as benign (Huckfeldt et al., 2016). In contrast, the diversity of phenotype–genotype correlations in STGD1, including asymptomatic cases due to combinations of mild *ABCA4* variants, may also explain the discrepancy between cumulative carrier frequency and clinical reporting of *ABCA4*-related retinal dystrophy.

4.3 | The novel shared maternal deletion-insertion allele

Bioinformatic prediction of the novel *ABCA4* c.6031_6044delins18^{M}/p.(Ile2003LeufsTer41) variant, later confirmed by transcript analysis, showed activation of a cryptic splice acceptor site that leads to a shift in reading frame and the introduction of a premature termination codon (p.Ile2003LeufsTer41) in the NBD2 of the C-terminal half of the ABCA4 protein. According to our results, the occurrence of the premature termination codon in exon 45 would render these transcripts susceptible to NMD but ultimately the loss of amino acids within and beyond the NBD2 domain compromises the functional protein (Figure 5). Since studies of the tissue-specific pattern of *ABCA4* splicing are not included in this work, further research is needed to show the predominant consequences of this delins variant in various tissues, particularly in the retina. Future transcript studies using an NMD inhibitor may provide a more accurate estimation of the percentage of *ABCA4* transcripts that undergo NMD due to the delins variant in different cells. The truncated protein translated from the shorter transcripts is produced with the deletion of a significant "VFVNFA" motif, present in the last 30–35 amino acids of NBD2. This motif is highly conserved not only among several members of the ABC transporter superfamily, but also highly conserved in phylogeny between species (Fitzgerald et al., 2004; Stenirri et al., 2006). Previous reports showed that alteration of the

"VFVNFA" motif eliminated the binding of apolipoproteinA-I and affected the lipid efflux activity of *ABCA1*, a member of the A-subclass of ABC proteins that has the highest amino acid homology with ABCA7 (54%) and the retina-specific ABCA4 (52%), respectively (Kaminski, Piehler, & Wenzel, 2006). The chimeric transporters generated by substituting the C-terminus of the ABCA1 protein with the C-terminus of ABCA4, containing the "VFVNFA" motif, have been shown to be functional proteins. However, substitution of the C-terminus of ABCA7, lacking the "VFVNFA" motif, did not produce an active protein (Fitzgerald et al., 2004). Frameshift mutations, c.6184_6187delGTCT (Wangtiraumnuay, Capasso, Tsukikawa, Levin, & Biswas-Fiss, 2018), c.6707delTCACACAG (Webster et al., 2001), and c.6710insA (Yatsenko et al., 2001) affecting the motifs found in the C-terminus of the ABCA4 protein have been identified as pathogenic in patients affected by STGD1. These mutations lead to disruptions of the "VFVNFA" motif and are predicted to compromise ABCA4 protein function. Additionally, a patient carrying the first reported de novo 44-bp deletion in the *ABCA4* gene that causes skipping of exon 49, coding for the "VFVNFA" motif, has been diagnosed with cone-rod dystrophy (Stenirri et al., 2006), which sheds new insight into the function of the last 30 amino acids of the ABCA4 protein.

To our knowledge, this is the first report to evaluate the aberrant splicing consequences of a delins variant of *ABCA4* using STGD1 patient-derived fibroblasts. We have provided experimental evidence that the c.6031_6044delins18^{M}/p.(Ile2003LeufsTer41) variant must be classified as a "pathogenic" variant, based on the ACMG/AMP guidelines. However, the effect of c.6031_6044delins18^{M}/p.(Ile2003LeufsTer41) on the splicing process cannot be further validated, as we have not found any other STGD1 individuals carrying this variant so far. Although patient-derived fibroblasts can be used to evaluate splicing defects of a retina-specific gene shown by our group and others (Aukrust et al., 2017; Sangermano et al., 2019), evaluation of the *ABCA4* variants in patient-derived retinal cells are likely to be essential, particularly for *ABCA4* variants that alter splicing.

In conclusion, an STGD1 family with pseudodominant transmission and intrafamilial phenotypic variability was described. Using STGD1 patient-derived fibroblasts, we revealed that a novel *ABCA4* c.6031_6044delins18^{M}/p.(Ile2003LeufsTer41) variant resulted in a partial deletion of exon 44 due to activation of a cryptic splice acceptor site, resulting in a severe, pathogenic *ABCA4* variant.

CONFLICT OF INTEREST

The authors have nothing to disclose.

AUTHOR'S CONTRIBUTION

All authors made substantial contributions to this study and approved the final version of the manuscript. Below is the contribution of each author to the manuscript: Di Huang performed transcript analyses and drafted the manuscript with input from all co-authors. Jennifer A. Thompson was involved in the genetic and pathogenicity analyses, and generated the table of pathogenicity assessment data. Jason Charng contributed to image processing, image analysis, and generated figures of clinical investigations. Shang-Chih Chen, Dana Zhang, and Abbie Adams conducted the dermal fibroblast culture. Enid Chelva, Terri L. McLaren, Tina M. Lamey, and John N. De Roach contributed to the establishment and management of the Australian Inherited Retinal Disease Registry & DNA Bank. Ian J. Constable and Fred K. Chen contributed to the clinical characterization of the reported family. Samuel McLenachan, May Thandar Aung-Htut, Sue Fletcher, and Steve D. Wilton critically revised the manuscript for important intellectual content. Fred K. Chen interpreted ophthalmic imaging data, recruited the family members into the natural history study, funded this research program to facilitate skin tissue collection and biobank, and provided oversight to the project.

DATA AVAILABILITY STATEMENT

Data sharing is not applicable to this article as no new data were created or analyzed in this study.

ORCID

Di Huang https://orcid.org/0000-0001-5657-0625
Jennifer A. Thompson https://orcid.org/0000-0003-3553-6457
Jason Charng https://orcid.org/0000-0002-5778-6310
Enid Chelva https://orcid.org/0000-0001-6603-2548
Samuel McLenachan https://orcid.org/0000-0001-5732-7387
Shang-Chih Chen https://orcid.org/0000-0002-5746-6982
Dan Zhang https://orcid.org/0000-0003-1728-9069
Terri L. McLaren https://orcid.org/0000-0003-3195-669X
Tina M. Lamey https://orcid.org/0000-0002-4608-4073
Ian J. Constable https://orcid.org/0000-0002-2140-6478
John N. De Roach https://orcid.org/0000-0002-2682-5380
May Thandar Aung-Htut https://orcid.org/0000-0002-6379-2303
Abbie Adams https://orcid.org/0000-0003-3445-7052
Sue Fletcher https://orcid.org/0000-0002-8632-641X
Steve D. Wilton https://orcid.org/0000-0002-9400-893X
Fred K. Chen https://orcid.org/0000-0003-2809-9930

REFERENCES

Albert, S., Garanto, A., Sangermano, R., Khan, M., Bax, N. M., Hoyng, C. B., … Cremers, F. P. M. (2018). Identification and rescue of splice defects caused by two neighboring deep-intronic ABCA4 mutations underlying Stargardt disease. *American Journal of Human Genetics*, *102*(4), 517–527. https://doi.org/10.1016/j.ajhg.2018.02.008

Allikmets, R., Singh, N., Sun, H., Shroyer, N. F., Hutchinson, A., Chidambaram, A., … Lupski, J. R. (1997). A photoreceptor cell-specific ATP-binding transporter gene (ABCR) is mutated in recessive Stargardt macular dystrophy. *Nature Genetics*, *15*(3), 236–246. https://doi.org/10.1038/ng0397-236

Aukrust, I., Jansson, R. W., Bredrup, C., Rusaas, H. E., Berland, S., Jørgensen, A., … Knappskog, P. M. (2017). The intronic ABCA4 c.5461-10T>C variant, frequently seen in patients with Stargardt disease, causes splice defects and reduced ABCA4 protein level. *Acta Ophthalmologica*, *95*(3), 240–246.

Bach, M., Brigell, M. G., Hawlina, M., Holder, G. E., Johnson, M. A., McCulloch, D. L., … Viswanathan, S. (2013). ISCEV standard for clinical pattern electroretinography (PERG): 2012 update. *Documenta Ophthalmologica*, *126*(1), 1–7. https://doi.org/10.1007/s10633-012-9353-y

Braun, T. A., Mullins, R. F., Wagner, A. H., Andorf, J. L., Johnston, R. M., Bakall, B. B., … Stone, E. M. (2013). Non-exomic and synonymous variants in ABCA4 are an important cause of Stargardt disease. *Human Molecular Genetics*, *22*(25), 5136–5145. https://doi.org/10.1093/hmg/ddt367

Cartegni, L., Wang, J., Zhu, Z., Zhang, M. Q., & Krainer, A. R. (2003). ESEfinder: A web resource to identify exonic splicing enhancers. *Nucleic Acids Research*, *31*(13), 3568–3571. https://doi.org/10.1093/nar/gkg616

Chiang, J. P., Lamey, T., McLaren, T., Thompson, J. A., Montgomery, H., & De Roach, J. (2015). Progress and prospects of next-generation sequencing testing for inherited retinal dystrophy. *Expert Review of Molecular Diagnostics*, *15*(10), 1269–1275. https://doi.org/10.1586/14737159.2015.1081057

Constable, P. A., Bach, M., Frishman, L. J., Jeffrey, B. G., & Robson, A. G.; International Society for Clinical Electrophysiology of Vision. (2017). ISCEV Standard for clinical electro-oculography (2017 update). *Documenta Ophthalmologica*, *134*(1), 1–9. https://doi.org/10.1007/s10633-017-9573-2

Cremers, F. P., van de Pol, D. J., van Driel, M., den Hollander, A. I., van Haren, F. J., Knoers, N. V., … Hoyng, C. B. (1998). Autosomal recessive retinitis pigmentosa and cone-rod dystrophy caused by splice site mutations in the Stargardt's disease gene ABCR. *Human Molecular Genetics*, *7*(3), 355–362. https://doi.org/10.1093/hmg/7.3.355

De Roach, J. N., McLaren, T. L., Paterson, R. L., O'Brien, E. C., Hoffmann, L., Mackey, D. A., … Lamey, T. M. (2013).

Establishment and evolution of the Australian Inherited Retinal Disease Register and DNA Bank. *Clinical and Experimental Ophthalmology*, *41*(5), 476–483. https://doi.org/10.1111/ceo.12020

DeLano, W. L. (2002). Pymol: An open-source molecular graphics tool. *CCP4 Newsletter On Protein Crystallography*, *40*(1), 82–92.

den Dunnen, J. T. (2016). Sequence variant descriptions: HGVS nomenclature and mutalyzer. *Current Protocols in Human Genetics*, *90*, 7.13.1–17.13.19. https://doi.org/10.1002/cphg.2

Fishman, G. A., Stone, E. M., Grover, S., Derlacki, D. J., Haines, H. L., & Hockey, R. R. (1999). Variation of clinical expression in patients with Stargardt dystrophy and sequence variations in the ABCRGene. *Archives of Ophthalmology*, *117*(4), 504–510. https://doi.org/10.1001/archopht.117.4.504

Fitzgerald, M. L., Okuhira, K., Short, G. F. 3rd, Manning, J. J., Bell, S. A., & Freeman, M. W. (2004). ATP-binding cassette transporter A1 contains a novel C-terminal VFVNFA motif that is required for its cholesterol efflux and ApoA-I binding activities. *Journal of Biological Chemistry*, *279*(46), 48477–48485. https://doi.org/10.1074/jbc.M409848200

Huckfeldt, R. M., East, J. S., Stone, E. M., & Sohn, E. H. (2016). Phenotypic variation in a family with pseudodominant Stargardt disease. *JAMA Ophthalmology*, *134*(5), 580–583. https://doi.org/10.1001/jamaophthalmol.2015.5471

Jaakson, K., Zernant, J., Kulm, M., Hutchinson, A., Tonisson, N., Glavac, D., … Allikmets, R. (2003). Genotyping microarray (gene chip) for the ABCR (ABCA4) gene. *Human Mutation*, *22*(5), 395–403. https://doi.org/10.1002/humu.10263

Kaminski, W. E., Piehler, A., & Wenzel, J. J. (2006). ABC A-subfamily transporters: Structure, function and disease. *Biochimica et Biophysica Acta (BBA) - Molecular Basis of Disease*, *1762*(5), 510–524. https://doi.org/10.1016/j.bbadis.2006.01.011

Lambertus, S., van Huet, R. A. C., Bax, N. M., Hoefsloot, L. H., Cremers, F. P. M., Boon, C. J. F., … Hoyng, C. B. (2015). Early-onset stargardt disease: Phenotypic and genotypic characteristics. *Ophthalmology*, *122*(2), 335–344. https://doi.org/10.1016/j.ophtha.2014.08.032

Lee, W., Xie, Y., Zernant, J., Yuan, B. O., Bearelly, S., Tsang, S. H., … Allikmets, R. (2016). Complex inheritance of ABCA4 disease: Four mutations in a family with multiple macular phenotypes. *Human Genetics*, *135*(1), 9–19. https://doi.org/10.1007/s00439-015-1605-y

Lois, N., Holder, G. E., Fitzke, F. W., Plant, C., & Bird, A. C. (1999). Intrafamilial variation of phenotype in Stargardt macular dystrophy-Fundus flavimaculatus. *Investigative Ophthalmology and Visual Science*, *40*(11), 2668–2675.

Maugeri, A., Klevering, B. J., Rohrschneider, K., Blankenagel, A., Brunner, H. G., Deutman, A. F., … Cremers, F. P. M. (2000). Mutations in the ABCA4 (ABCR) gene are the major cause of autosomal recessive cone-rod dystrophy. *American Journal of Human Genetics*, *67*(4), 960–966. https://doi.org/10.1086/303079

McCulloch, D. L., Marmor, M. F., Brigell, M. G., Hamilton, R., Holder, G. E., Tzekov, R., & Bach, M. (2015). ISCEV Standard for full-field clinical electroretinography (2015 update). *Documenta Ophthalmologica*, *130*(1), 1–12. https://doi.org/10.1007/s10633-014-9473-7

Molday, R. S., Zhong, M., & Quazi, F. (2009). The role of the photoreceptor ABC transporter ABCA4 in lipid transport and Stargardt macular degeneration. *Biochimica et Biophysica Acta (BBA) - Molecular and Cell Biology of Lipids*, *1791*(7), 573–583. https://doi.org/10.1016/j.bbalip.2009.02.004

Paavo, M., Lee, W., Allikmets, R., Tsang, S., & Sparrow, J. R. (2019). Photoreceptor cells as a source of fundus autofluorescence in recessive Stargardt disease. *Journal of Neuroscience Research*, *97*(1), 98–106. https://doi.org/10.1002/jnr.24252

Pertea, M., Lin, X., & Salzberg, S. L. (2001). GeneSplicer: A new computational method for splice site prediction. *Nucleic Acids Research*, *29*(5), 1185–1190. https://doi.org/10.1093/nar/29.5.1185

Quazi, F., Lenevich, S., & Molday, R. S. (2012). ABCA4 is an N-retinylidene-phosphatidylethanolamine and phosphatidylethanolamine importer. *Nature Communications*, *3*, 925. https://doi.org/10.1038/ncomms1927

Reese, M. G., Eeckman, F. H., Kulp, D., & Haussler, D. (1997). Improved splice site detection in Genie. *Journal of Computational Biology*, *4*(3), 311–323. https://doi.org/10.1089/cmb.1997.4.311

Richards, S., Aziz, N., Bale, S., Bick, D., Das, S., Gastier-Foster, J., … Rehm, H. L. (2015). Standards and guidelines for the interpretation of sequence variants: A joint consensus recommendation of the American College of Medical Genetics and Genomics and the Association for Molecular Pathology. *Genetics in Medicine*, *17*(5), 405–424. https://doi.org/10.1038/gim.2015.30

Runhart, E. H., Sangermano, R., Cornelis, S. S., Verheij, J., Plomp, A. S., Boon, C. J. F., … Cremers, F. P. M. (2018). The common ABCA4 variant p.Asn1868Ile shows nonpenetrance and variable expression of Stargardt disease when present in trans with severe variants. *Investigative Ophthalmology and Visual Science*, *59*(8), 3220–3231. https://doi.org/10.1167/iovs.18-23881

Sangermano, R., Garanto, A., Khan, M., Runhart, E. H., Bauwens, M., Bax, N. M., … Cremers, F. P. M. (2019). Deep-intronic ABCA4 variants explain missing heritability in Stargardt disease and allow correction of splice defects by antisense oligonucleotides. *Genetics in Medicine*, *21*(8), 1751–1760. https://doi.org/10.1038/s41436-018-0414-9

Schindler, E. I., Nylen, E. L., Ko, A. C., Affatigato, L. M., Heggen, A. C., Wang, K., … Stone, E. M. (2010). Deducing the pathogenic contribution of recessive ABCA4 alleles in an outbred population. *Human Molecular Genetics*, *19*(19), 3693–3701. https://doi.org/10.1093/hmg/ddq284

Schulz, H. L., Grassmann, F., Kellner, U., Spital, G., Ruther, K., Jagle, H., … Stohr, H. (2017). Mutation spectrum of the ABCA4 gene in 335 Stargardt disease patients from a multicenter German cohort-impact of selected deep intronic variants and common SNPs. *Investigative Ophthalmology and Visual Science*, *58*(1), 394–403. https://doi.org/10.1167/iovs.16-19936

Schwarz, J. M., Cooper, D. N., Schuelke, M., & Seelow, D. (2014). MutationTaster2: Mutation prediction for the deep-sequencing age. *Nature Methods*, *11*(4), 361–362. https://doi.org/10.1038/nmeth.2890

Stargardt, K. (1909). Über familiäre, progressive degeneration in der maculagegend des auges. *Albrecht von Graefes Arch Klin Ophthalmology*, *71*, 534–550. https://doi.org/10.1007/BF01961301

Stenirri, S., Battistella, S., Fermo, I., Manitto, M. P., Martina, E., Brancato, R., … Cremonesi, L. (2006). De novo deletion removes a conserved motif in the C-terminus of ABCA4 and results in cone-rod dystrophy. *Clinical Chemistry and Laboratory Medicine*, *44*(5), 533–537. https://doi.org/10.1515/CCLM.2006.116

Tanna, P., Strauss, R. W., Fujinami, K., & Michaelides, M. (2017). Stargardt disease: Clinical features, molecular genetics, animal models and therapeutic options. *British Journal of Ophthalmology*, *101*(1), 25–30. https://doi.org/10.1136/bjophthalmol-2016-308823

Thompson, J. A., De Roach, J. N., McLaren, T. L., Montgomery, H. E., Hoffmann, L. H., Campbell, I. R., … Lamey, T. M. (2017). The genetic profile of Leber congenital amaurosis in an Australian cohort. *Molecular Genetics and Genomic Medicine*, 5(6), 652–667. https://doi.org/10.1002/mgg3.321

Wangtiraumnuay, N., Capasso, J., Tsukikawa, M., Levin, A., & Biswas-Fiss, E. (2018). Novel ABCA4 mutation leads to loss of a conserved C-terminal motif: Implications for predicting pathogenicity based on genetic testing. *European Journal of Ophthalmology*, 28(1), 123–126. https://doi.org/10.5301/ejo.5001019

Webster, A. R., Héon, E., Lotery, A. J., Vandenburgh, K., Casavant, T. L., Oh, K. T., … Levin, A. (2001). An analysis of allelic variation in the ABCA4 gene. *Investigative Ophthalmology and Visual Science*, 42(6), 1179–1189.

Westeneng-van Haaften, S. C., Boon, C. J., Cremers, F. P., Hoefsloot, L. H., den Hollander, A. I., & Hoyng, C. B. (2012). Clinical and genetic characteristics of late-onset Stargardt's disease. *Ophthalmology*, 119(6), 1199–1210. https://doi.org/10.1016/j.ophtha.2012.01.005

Wilton, S. D., Lim, L., Dye, D., & Laing, N. (1997). Bandstab: A PCR-based alternative to cloning PCR products. *BioTechniques*, 22(4), 642–645. https://doi.org/10.2144/97224bm14

Yatsenko, A. N., Shroyer, N. F., Lewis, R. A., & Lupski, J. R. (2001). Late-onset Stargardt disease is associated with missense mutations that map outside known functional regions of ABCR (ABCA4). *Human Genetics*, 108(4), 346–355.

Yeo, G., & Burge, C. B. (2004). Maximum entropy modeling of short sequence motifs with applications to RNA splicing signals. *Journal of Computational Biology*, 11(2–3), 377–394. https://doi.org/10.1089/1066527041410418

Zaneveld, J., Siddiqui, S., Li, H., Wang, X., Wang, H., Wang, K., … Chen, R. (2015). Comprehensive analysis of patients with Stargardt macular dystrophy reveals new genotype-phenotype correlations and unexpected diagnostic revisions. *Genetics in Medicine*, 17(4), 262–270. https://doi.org/10.1038/gim.2014.174

Zernant, J., Lee, W., Collison, F. T., Fishman, G. A., Sergeev, Y. V., Schuerch, K., … Allikmets, R. (2017). Frequent hypomorphic alleles account for a significant fraction of ABCA4 disease and distinguish it from age-related macular degeneration. *Journal of Medical Genetics*, 54(6), 404–412. https://doi.org/10.1136/jmedgenet-2017-104540

Zernant, J., Lee, W., Nagasaki, T., Collison, F. T., Fishman, G. A., Bertelsen, M., … Allikmets, R. (2018). Extremely hypomorphic and severe deep intronic variants in the ABCA4 locus result in varying Stargardt disease phenotypes. *Cold Spring Harbor Molecular Case Studies*, 4(4), a002733. https://doi.org/10.1101/mcs.a002733

Zernant, J., Schubert, C., Im, K. M., Burke, T., Brown, C. M., Fishman, G. A., … Allikmets, R. (2011). Analysis of the ABCA4 gene by next-generation sequencing. *Investigative Ophthalmology and Visual Science*, 52(11), 8479–8487. https://doi.org/10.1167/iovs.11-8182

Zernant, J., Xie, Y. A., Ayuso, C., Riveiro-Alvarez, R., Lopez-Martinez, M.-A., Simonelli, F., … Allikmets, R. (2014). Analysis of the ABCA4 genomic locus in Stargardt disease. *Human Molecular Genetics*, 23(25), 6797–6806. https://doi.org/10.1093/hmg/ddu396

Zhang, M. Q. (1998). Statistical features of human exons and their flanking regions. *Human Molecular Genetics*, 7(5), 919–932. https://doi.org/10.1093/hmg/7.5.919

Zhang, Y. (2008). I-TASSER server for protein 3D structure prediction. *BMC Bioinformatics*, 9, 40. https://doi.org/10.1186/1471-2105-9-40

SUPPORTING INFORMATION

Additional supporting information may be found online in the Supporting Information section.

How to cite this article: Huang D, Thompson JA, Charng J, et al. Phenotype–genotype correlations in a pseudodominant Stargardt disease pedigree due to a novel *ABCA4* deletion–insertion variant causing a splicing defect. *Mol Genet Genomic Med*. 2020;8:e1259. https://doi.org/10.1002/mgg3.1259